The Primary Antibody Repertoire Represents a Linked Network of Degenerate Antigen Specificities[1]

Venkatasamy Manivel,* Fahri Bayiroglu,* Zaved Siddiqui,* Dinakar M. Salunke,† and Kanury V. S. Rao[2]*

In this study, germline Abs were used to select clones from a random dodecapeptide phage-display library. This revealed a much greater heterogeneity of binders than could be obtained with mutated daughter Abs that presumably had been selected in vivo by nominal Ag during active immune responses. We demonstrate that the pluripotency of germline Abs can subsequently be optimized by binding interactions that correlate with thermodynamic changes indicative of structural adaptations at the interface. This singular feature confers on each Ab a distinct window of Ag specificities, where the entropic space explored constitutes a thermodynamic signature of that particular Ab. Combining site plasticity may facilitate overlaps in such windows, with independent Abs converging onto common determinants with near identical binding affinities. In addition to providing for an amplified recognition potential, this networking of individual spectra of Ag specificities simultaneously facilitates the rapid recognition of Ag. Importantly, it also ensures that the primary response is composed of Abs with a high degree of "evolvability." ***The Journal of Immunology*****, 2002, 169: 888–897.**

The central postulate of the clonal selection theory (1) of one lymphocyte, one Ab, has widely been interpreted to signify that each lymphocyte expresses a unique Ag-combining site. Consequently, explanations for the diversity of humoral responses have generally emphasized the combinatorial and somatic mutational processes that lead to the genetic diversity of the Ab repertoire (2, 3). Emerging data, however, appear to question this basic assumption and, in fact, provoke a paradigm shift in our perception of how Ag recognition is actually achieved in an immune response.

Accumulating evidence is now beginning to favor the view that the Ag recognition function of the adaptive immune system is mediated by the use of flexible modules. For instance, studies have demonstrated that the germline Abs undergo a substantial structural change in the course of binding to an Ag (4–6). This has been interpreted to reflect adaptability at the level of the combining site (4, 5). Similarly, structural plasticity for the combining site of the TCR has also been suggested, based on the observation of induced fit mechanisms, governing its interaction with the cognate peptide-MHC complex (7–9).

Although the existence of pliable Ag-combining sites is now established, their relevance to the functioning of the adaptive immune system remains to be validated. This is equally true of the earlier proposal that combining site plasticity may confer cross-reactivity to Ag receptors, thereby rendering them capable of recognizing more than one Ag (4, 5, 9–11). Whether such a property eventually proves beneficial to immune function would largely depend upon the degree of plasticity inherent to such a combining site. Thus, if cross-reactivity of individual naive Ag receptors were to be restricted to closely related antigenic structures, the net gain—in terms of immune recognition—can be expected to be only incremental.

It was with the intent of addressing these and related issues that the present study was undertaken. By using a phage-display library of random dodecapeptides and a panel of independent Abs, we demonstrate that each germline Ab can indeed bind to a large variety of unrelated antigenic determinants. Binding predominantly occurred through entropy-enthalpy compensatory mechanisms leading, contrary to expectations, to a relatively clustered range of physiologically permissive binding affinities. Importantly, paratope plasticity also allowed for a convergence of specificities, with independent Abs recognizing a common subset of antigenic determinants. Thus, although on the one hand receptor flexibility markedly amplifies the recognition repertoire, by networking independent receptor specificities on the other, it also provides a mode by which recognition of Ag is rapidly achieved.

Materials and Methods

Monoclonal Abs

The anti-(4-hydroxy-3-nitrophenyl)-acetyl (anti-NP)[3] hybridomas BBE6.12H3 and Bg53-5, and the anti-*p*-azophenylarsonate (anti-Ars) hybridomas 36-65 and 36-71 were a kind gift from Dr. T. Manser (Kimmel Cancer Institute, Philadelphia, PA), whereas the anti-peptide hybridoma PC7bM has been described earlier (12). All of these mAbs were first obtained as ascites and then purified by affinity chromatography as described earlier (5). When necessary, the IgM class mAb PC7bM was subsequently converted to its monomeric form by reductive alkylation as described earlier (12). For mAb 36-65, the amino acid sequences of the complementarity-determining region 3 of the H chain (HCDR3) and complementarity-determining region 3 of the L chain (LCDR3) are SVYYGGSYYFDY and QQGNTLPRT, respectively. The corresponding sequences for mAb BBE6.12H3 are YDYYGSSYFDY (HCDR3), and ALWYSNHWV (LCDR3); for mAb PC7bM, these are QRTIGTPGAY (HCDR3) and

*Immunology Group, International Center for Genetic Engineering and Biotechnology, and †National Institute of Immunology, Aruna Asaf Ali Marg, New Delhi, India

Received for publication November 20, 2001. Accepted for publication May 9, 2002.

The costs of publication of this article were defrayed in part by the payment of page charges. This article must therefore be hereby marked *advertisement* in accordance with 18 U.S.C. Section 1734 solely to indicate this fact.

[1] This work was supported by funds from the International Center for Genetic Engineering and Biotechnology (Italy) and Department of Biotechnology, Government of India.

[2] Address correspondence and reprint requests to Dr. Kanury V. S. Rao, Immunology Group, International Center for Genetic Engineering and Biotechnology, Aruna Asaf Ali Marg, New Delhi 110 067, India. E-mail address: kanury@icgeb.res.in

[3] Abbreviations used in this paper: NP, (4-hydroxy-3-nitrophenyl)-acetyl; HCDR3, complementarity-determining region 3 of the H chain; LCDR3, complementarity-determining region 3 of the L chain; m, membrane; Ars, *p*-azophenylarsonate; BCR, B cell receptor.

0022-1767/02/$02.00

QHIREAYT (LCDR3). The $V_\kappa L$ genes for mAbs 36-65 and PC7bM belonged to subgroups V and III, respectively, whereas mAb BBE6.12H3 uses a λ1 L chain.

Purified IgG Abs were digested with papain to generate Fab products using an established protocol (13). The IgM mAb was first digested with pepsin (37°C, 16 h), followed by reduction with DTT (14). The resultant Fab were then resolved by passing through a Sephadex G-200 (fine) (Pharmacia Biotech, Uppsala, Sweden) column and concentrated to ~5 mg/ml, and purity was ascertained by SDS-PAGE.

Analysis of Ab cross-reactivity

This was essentially achieved using the Ph.D.-12 Phage Display Peptide Library kit, which displays randomly generated linear peptides of 12 residues (New England Biolabs, Cambridge, MA). This library expresses a repertoire of 2×10^9 random peptide 12-mers fused to the minor coat protein (pIII) of M13 phage, with between three and five copies of the insert sequence per phage. The displayed peptide 12-mers are expressed at the N terminus of pIII, where the first residue of the mature protein is the first randomized position. The peptide is followed by a short spacer (GGGS) and then the wild-type pIII sequence.

Aliquots of the above library were first subjected to three rounds of selection, in solution, against 100 nM final concentrations of either mAb BBE6.12H3 or mAb 36-65, strictly following the recommended protocol of the manufacturer. Briefly, the library was incubated with mAb in a total volume of 200 μl for 1 h at room temperature. Subsequent to this, bound complexes were then separated by first incubating with protein G-Sepharose (at room temperature for 15 min), followed by centrifugation. The pellet was washed (10×1 ml) with TBS (pH 7.5) containing 0.1% Tween 20. To minimize nonspecific reactivities, preadsorption against nonspecific mouse IgG followed by protein G-Sepharose (blocked with BSA) first preceded each round of selection. Furthermore, at the end of each selection cycle, only specifically bound phage was eluted by competitive displacement with a 10-fold molar excess (2 μM based on a valency of 2/Ab molecule) of the homologous Ag (i.e., either NP_{23}-BSA or Ars-BSA). Next, individual phage clones were amplified and the insert was identified by nucleotide sequencing.

For an examination of convergent reactivities, the mAb BBE6.12H3-specific phage pool obtained above was subjected to two additional rounds of screening against mAb 36-65 (pool BBE6/36-65). Here again, bound phage was eluted with Ars-BSA, and individual clones were subsequently amplified. The above pool BBE6/36-65 was also taken, after a prescreen with biotinylated mouse IgM, for further selection against monomeric mAb PC7bM (two rounds). For this, biotinylated Ab was used, and the immune complexes were separated using streptavidin-agarose. Bound phage was eluted by incubation with a 10-fold excess of the homologous peptide Ag, PS1CT3 (12). For binding analysis, all individual clones were amplified to titers of between 10^{13} and 3×10^{17} PFU/ml, and then they were either biotinylated for surface plasmon resonance studies or derivatized with FITC for analysis of binding to M12 cells.

Several control experiments were performed with the above to ensure the validity and specificity of our screening procedure. For example, each round of selection and elution with a given germline Ab was always accompanied by a parallel group, where the corresponding affinity-matured derivative (e.g., mAb 36-71 for mAb 36-65 or mAb Bg53-5 for BBE6.12H3) was included instead. Titers that were significantly less than 10^2 PFU/ml were routinely obtained from these latter groups, confirming the germline mAb-dependent specificity of our protocol. A subset ($n = 10$) of the phage clones selected by the affinity-matured mAbs was also processed further to determine the affinity of their binding to the selecting mAb. Such experiments yielded K_d values ranging from 200 to 400 μM, providing a rough estimate of the low-affinity cutoff of our selection protocol. Finally, although mAb-bound phage clones were eluted by competitive displacement with excess of the homologous Ag, we consistently monitored the efficiency of this procedure at each step. For this, after the elution step, the mAbs were incubated with glycine-HCl (pH 2.7, 15 min at room temperature), after which the supernatants were neutralized and processed for the estimation of any residual phage titers. Such a comparison indicated that >95% of the bound phage was consistently eluted by our competitive displacement procedure. Thus, the protocol described above is specific and does not introduce any significant sampling bias.

Ab binding analysis

Ab-phage interactions were monitored by the technique of surface plasmon resonance on an Iasys Auto$^+$ instrument (Affinity Sensors, Cambridge, U.K.). Here, biotinylated cuvettes were used where streptavidin was first bound, followed by immobilization of individual biotinylated phage clones. Preliminary experiments indicated that optimal results were achieved when the amount of phage immobilized was between 1.3 and 2.4 ng/mm^2. Consequently, this range was retained for all analyses.

For the determination of K_d values, binding was examined at multiple Fab concentrations ranging from 5-fold above to ~5-fold below preliminary estimates for each mAb-phage interaction. Furthermore, binding analyses were performed at multiple temperatures of 20, 25, 30, and 35°C. Associations were monitored over a period of 7 to 12 min, whereas dissociations were followed over a 5-min period. Kinetic analysis was performed using the FASTfit software provided by the manufacturer, which yielded the k_{on} and k_{diss} at each Ab concentration and temperature. Second order rate constants (k_{ass}) at each temperature were then obtained from a linear regression plot of k_{on}, at that temperature, vs Ab concentration. The equilibrium K_d at 25°C was calculated for each interaction from the following equation: $K_d = k_{diss}/k_{ass}$. The stability of the Fab at the higher temperature (35°C) was ascertained as described earlier (5).

Generation of membrane $IgD_{H\text{-}\lambda L}$ ($mIgD_{H\text{-}\lambda L}$) transfected M12 cells

The entire λ_L and the variable IgH segment (including the leader sequence in both cases) was obtained by RT-PCR of the mRNA obtained from the BBE6.12H3 hybridoma cells. In parallel, resting B cells were isolated from BALB/c mouse splenocytes, and the resultant mRNA was taken for generation of the mIgD constant region by RT-PCR. The variable IgH and mIgD constant regions were then ligated and cloned into the pGEMT vector, and the integrity of the full-length cDNA was verified by nucleotide sequencing. Both the resultant λ_L and mIgD cDNAs were independently cloned into the retroviral vector PLNCX-2 (Clontech Laboratories, Palo Alto, CA). These constructs were then separately taken to infect packaging cells (Retropak PT67; Clontech) using a protocol recommended by the supplier. Supernatants from these two cultures were pooled in equal amounts and used in two rounds of transfection of M12 cells (15), again using the suggested protocol of the supplier. Stably transfected cells were selected on the basis of G418 resistance and were expanded before use.

Results

Cross-reactivity of select germline Abs

To evaluate cross-reactivity, we selected two germline mAbs for the present study. Both of these have been described earlier and include mAb 36-65, which was generated against the hapten Ars (16, 17). The second Ab used, mAb BBE6.12H3, was directed against the hapten NP (18). The H chain variable region of mAb 36-65 has been shown to be constructed from V_H J558, D_H Fl16.1, and J_H2 gene segments, whereas that of mAb BBE6.12H3 consists of V_H 186.2, D_H Fl16.1 and J_H2 (17, 18). In addition to this, the two mAbs are also distinguished on the basis of the H chain complementarity-determining region 3 (12 residues in 36-65 vs 11 amino acid residues in BBE6.12H3). Furthermore, whereas mAb 36-65 includes a L chain of the κ isotype, mAb BBE6.12H3 uses a λ L chain (17, 18). Thus, mAbs 36-65 and BBE6.12H3 represent structurally distinct Abs of independent origin.

We examined the cross-reactive potential of these two Abs by three rounds of selection against a phage display library of randomly generated dodecapeptides (see *Materials and Methods*). Of the numerous clones that were selected, 24–25—with distinct insert sequences—were taken for further analysis. The amino acid sequences of the inserts in these phages are given in Tables I and II, and it is evident within each panel that they show no significant similarity at either the level of sequence homology or overall chemical composition.

Binding properties of the two mAbs to each of the phage clones in the corresponding panel were further characterized by using the technique of surface plasmon resonance (see *Materials and Methods*). To eliminate any cooperative effects during either the association or the dissociation step of binding, we used the monovalent Fab, generated from both mAbs, for the binding analysis. Furthermore, specificity of the system was also established by the inclusion of several controls. First, whereas binding to individual phage clones was obtained with the appropriate germline Fab, no reactivity was detected, however, when Fab from the corresponding

Table I. *Cross-reactivity of mAb 36-65*[a]

Clone No.	Insert Sequence	K_d (μM)	k_{ass} ($M^{-1}s^{-1}$) ($\times 10^{-5}$)	k_{diss} (s^{-1}) ($\times 10^{2}$)	ΔG_{eq} kJM^{-1}
65-04.01	FHKPNHHRPAFA	1.05	0.39	4.10	−34.36
65-37.18	RLLIADPPSPRE	0.15	0.37	0.55	−38.87
65-04.11	HHWTPNEAYHRT	0.78	0.19	1.47	−34.94
65-37.28	KLASIPTHTSPL	0.12	0.37	0.44	−40.30
65-37.09	TPIMSHYSLGDF	0.77	0.21	1.66	−34.73
65-37.01	TLYKQYGPSIMP	0.40	0.13	0.66	−35.86
65-37.05	KDAAPTYSMSPN	0.94	0.04	3.50	−34.68
65-04.17	FYGPSNLSSPKP	0.40	0.90	0.81	−36.51
65-37.03	YHDGSSIQHLAS	1.53	0.12	1.84	−33.22
65-04.04	SLGDNLTNHNLR	0.21	0.17	0.35	−38.35
65-04.20	HTKYHSLPVYNS	1.70	0.15	2.60	−32.29
65-04.27	SPIQQIMHTSPM	3.10	0.06	1.90	−31.06
65-04.05	YSTHWWAVSSLS	0.48	0.14	0.68	−35.59
65-37.08	QQNNQMYNSLTK	1.10	0.06	0.66	−34.10
65-04.15	HARINPSFPLPI	3.02	0.04	1.10	−31.56
65-04.21	HYTNSQDASPRR	1.40	0.05	0.78	−31.23
65-37.23	KVATYPLTAARV	4.20	0.08	3.45	−30.79
65-37.26	RTSLHLSFPRLS	1.02	0.04	0.44	−34.35
65-04.25	ALAHYTHLSPNL	16.00	0.05	8.02	−26.99
65-04.08	YNPYNPAHRPRW	1.36	0.07	1.02	−33.59
65-04.23	DHPQIFREPLDG	5.30	0.04	2.20	−30.39
65-37.06	NDMPNGLLRPFS	0.50	0.07	0.34	−36.64
65-04.30	IIDRSQLHPVPS	3.47	0.06	2.10	−31.03
65-04.22	SLAQQEANSCPR	20.40	0.01	2.21	−26.89
65-37.20	FIQPMKKSHLQK	2.10	0.19	0.39	−32.59

[a] Binding properties of mAb 36-65 to the individual phage clones, selected as described in *Results*, are given here. Values for K_d, k_{ass}, and k_{diss} represent the mean of two independent determinations, on separately immobilized cuvettes (*Materials and Methods*), with the deviation from the mean being <40% in all cases. ΔG_{eq} was calculated using the mean values for k_{ass} and k_{diss} as described in *Results*. The insert sequence in each of the phage clones is also given. Of a total of 66 clones sequenced, the insert sequence corresponding to clone 65-04.04 occurred three times, whereas those representing clones 65-37.28, 65-04.05, 65-04.08, and 65-37.06 appeared twice. The remaining sequences were not repeated.

affinity-matured mAbs were used in parallel experiments (data not shown). The affinity-matured derivatives used here were mAb 36-71 for mAb 36-65 and mAb Bg53-5 for mAb BBE6.12H3 (17, 18). Second, no interpanel cross-reactivities were obtained either. In other words, mAb 36-65 did not show any significant reactivity with the phage clones in Table II, whereas mAb BBE6.12H3 displayed only very weak to insignificant reactivity with members of the panel in Table I. Finally, specificity of mAb-phage binding could also be demonstrated by the fact that these interactions could be markedly inhibited, in ELISA, by simultaneous addition of the homologous Ag (i.e., Ars-BSA for 36-65 and NP-BSA for BBE6.12H3; data not shown).

The individual values for the K_d, and the kinetic rate constants obtained from our above analyses are given in Tables I and II. As is evident, the binding affinities obtained are widely distributed and spread over either a 100-fold (for mAb 36-65) or a 400-fold (for mAb BBE6.12H3) range (Tables I and II). These values, nonetheless, are well within the range of physiological relevance—at least when compared with mAb binding to the native Ag. In parallel experiments, we determined the K_d of Fab of mAbs 36-65 and BBE6.12H3 for the respective native Ags, Ars-BSA and NP-BSA, to be 37.0 μM and 50.0 μM, respectively. In an earlier study we have shown that intact, unfragmented mAbs 36-65 and BBE6.12H3 bind their native Ags with K_d values of 8.0 and 23.0 μM, respectively (5).

Although distributed over a wide range, the majority of the K_d values obtained in Tables I and II were nonetheless found to cluster within a relatively narrow spectrum. This is shown in Fig. 1*A*. In the case of mAb 36-65 reactivities, ~84% of these were limited to within a 40-fold range of K_d values between 0.1 and 4.0 μM (Fig. 1*A*). For mAb BBE6.12H3, the corresponding proportion of bindings within this affinity range was 67% percent (Fig. 1*A*). Thus, contrary to intuitive expectations, recognition of diverse antigenic sequences by at least these two germline Abs does not necessarily entail a significant compromise in terms of the affinity of the individual binding interactions. Interestingly, the comparable binding affinities observed in either Table I or II did not always reflect identity at the level of the kinetic constants, implying a heterogeneity of binding modes.

Phage-mAb cross-reactivities predominantly reflect the outcome of entropy-enthalpy compensatory processes

Successful binding interactions are always accompanied by a net negative change in the Gibbs free energy of binding at equilibrium (ΔG_{eq}), where the extent of change directly determines binding affinity. The free energy changes that occur upon binding are, in turn, modulated by net changes in two thermodynamic parameters, enthalpy (ΔH) and entropy (ΔS).[4] The enthalpy term describes heat changes that take place due to interactions at the binding interface (19, 20). In contrast, entropy changes identify net conformational/stereochemical/structural perturbations that occur either within the interacting entities or in the surrounding solvent molecules (19, 20).

As the next step, therefore, we determined the relative contribution from the enthalpy and entropy parameters, again using the technique of surface plasmon resonance, as described earlier (5). Briefly, both k_{ass} and k_{diss} values of mAb binding to each phage

[4] The Gibbs free energy of binding at equilibrium (ΔG_{eq}) relates to the binding affinity by the following equation: $\Delta G_{eq} = RT\ln K_d$. Here, R represents the universal gas constant, and T the temperature in degrees Kelvin. The free energy changes that accompany a binding reaction at equilibrium are also defined by the following relationship: $\Delta G_{eq} = \Delta H_{eq} - T\Delta S_{eq}$. Both the enthalpy ($\Delta H_{eq}$) and the entropy ($T\Delta S_{eq}$) terms, at equilibrium, in turn reflect differences in these two parameters between the individual association and dissociation steps of the binding interaction.

Table II. *Cross-reactivity of mAb BBE6.12H3*[a]

Clone No.	Insert Sequence	K_d (μM)	k_{ass} ($M^{-1}s^{-1}$) ($\times 10^{-5}$)	k_{diss} (s^{-1}) ($\times 10^{2}$)	ΔG_{eq} kJM^{-1}
B6-07	YQLRPNAETLRF	0.26	0.22	0.59	−37.35
B6-03	GIPVIKPPLPPS	0.12	0.43	0.50	−40.13
B6-29	TLQNTHYVRSDK	2.10	0.20	4.26	−32.77
B6-08	HPLNSTNVKKQV	3.56	0.01	0.34	−31.20
B6-13	DLWTTAIPTIPS	0.38	0.11	0.41	−36.78
B6-19	ASTFAPANRTAP	0.24	0.30	0.73	−37.88
B6-09	YLVKPPIDKLKA	10.20	0.06	6.02	−29.17
B6-14	LPPWKHKTSGVA	43.70	0.04	17.50	−25.03
B6-04	VSRHRSWHPHDL	12.30	0.11	1.30	−28.85
B6-30	SDFRTHQSSGSH	9.02	0.04	3.90	−29.58
B6-16	TTWSHHLSSAGL	1.32	0.04	0.51	−32.49
B6-23	LLADTTHHRPWT	8.21	0.06	4.51	−29.17
B6-02	STWPAFRLFTNI	0.46	0.08	0.38	−35.29
B6-22	TTPPPTTHHSAR	3.41	0.04	1.36	−31.44
B6-01	GGQTMRTPTLLS	2.72	0.11	3.01	−31.85
B6-26	QTFAPMRGVTSL	9.74	0.04	3.81	−29.63
B6-11	MRADTTHHRPWT	2.52	0.05	1.12	−32.24
B6-39	GISRAPHALSAW	6.02	0.04	2.70	−29.93
B6-31	TKNTVSLPVGPG	2.90	0.05	0.15	−31.85
B6-35	NTLLHHRMPLPN	17.03	0.04	6.61	−27.50
B6-18	FTATTSHLIRRN	1.26	0.24	3.02	−33.97
B6-24	HAYTIKLWSPGH	2.42	0.06	1.53	−32.46
B6-17	SHPWNGEREISV	1.12	0.02	0.20	−34.2
B6-34	SGHHLLLNKMPN	5.20	0.05	2.72	−30.51

[a] Both the insert sequences of individual phage clones selected against mAb BBE6.12H3 as well as their binding properties to this mAb are given. The individual values shown were obtained as described for Table I. Of a total of 58 clones sequenced, the insert sequence derived from clone B6-09 appeared three times, whereas those derived from clones B6-16 and B6-24 were obtained twice. The remaining sequences were not repeated.

were determined as a function of increasing the temperature from 20 to 35°C. After this, the activation energy (Ea) for each association and dissociation step was determined from the slopes of the subsequent Arrhenius plots (ln $k_{ass/diss}$ vs 1/T). From these values, ΔH and $T\Delta S$ for the association and dissociation phases were then calculated using the following equations:

$$\Delta H_{ass/diss} = Ea - RT \quad (1)$$

$$\ln (k_{ass/diss}/T) = -\Delta H_{ass/diss}/RT + \Delta S_{ass/diss}/R + \ln (k'/h) \quad (2)$$

In equation 2, k' represents the Boltzman constant, whereas h denotes the Planck's constant. The values obtained from these equations were then taken to calculate ΔH_{eq}, $T\Delta S_{eq}$, and then ΔG_{eq}, as described earlier (5).[4] The ΔG_{eq} values obtained for mAb binding to each of the corresponding phage clones are given in Tables I and II and are validated by the fact that they correlate well with the observed binding affinities in all cases.

Plotted in Fig. 1, *B* and *C*, are the relative contributions from $T\Delta S_{eq}$ and ΔH_{eq} during the binding of either mAb 36-65 (Fig. 1*B*) or mAb BBE6.12H3 (Fig. 1*C*) to individual members of the respective phage panel. From an examination of the data in Fig. 1*B*, it is evident that multiple pathways operate during binding of mAb 36-65 to the various phage clones. In some of the cases (2 of 25), binding appears to be entropically driven, against an unfavorable contribution from enthalpy (Fig. 1*B*). In addition to this, there are also instances (6 of 25) where both components contribute favorably toward binding (Fig. 1*B*). The majority of the cases (17 of 25), however, describe a binding process that is enthalpically driven, against an increasing gradient of unfavorable entropy changes (Fig. 1*B*). Essentially similar results were also obtained for mAb BBE6.12H3, although entropy-enthalpy compensatory mechanisms accounted for all the bindings observed here (Fig. 1*C*). Although there were some examples of entropically driven binding (2 of 24), the overwhelming majority of cases (22 of 24) required compensation from enthalpy, to overcome the entropic penalty that accompanied the binding interaction (Fig. 1*C*).

The cumulative data in Fig. 1, *B* and *C*, therefore, reveal some important properties of the two germline Abs studied here. First, at

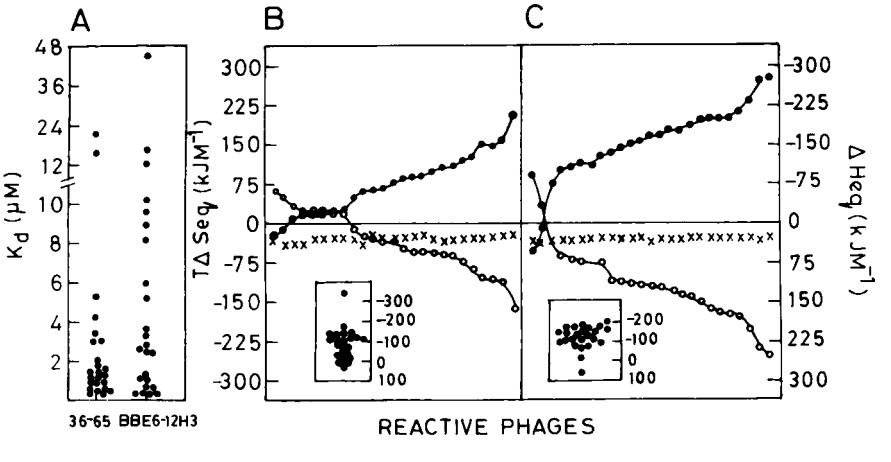

FIGURE 1. Cross-reactive properties of mAbs 36-65 and BBE6.12H3. *A*, Distribution of K_d values obtained for either Ab in Tables I and II, respectively. *B* and *C*, Relative contribution from ΔH_{eq} (●) and $T\Delta S_{eq}$ (○) to the overall free energy of binding (ΔG_{eq}, crosses) for each of the phage clones cross-reactive with either mAb 36-65 (*B*) or mAb BBE6.12H3 (*C*). These values were calculated from the mean k_{ass} and k_{diss} values of two separate experiments, performed on independently immobilized cuvettes, as described in *Results*. For both panels, the order of presentation from *left* to *right* is that of the phage clones listed from *top* to *bottom* in Tables I and II. The *inset* in both panels gives the distribution of $T\Delta S_{ass}$ obtained.

least in principle, cross-reactivity of the mAbs was facilitated by the fact that any of the three thermodynamically permissive routes (i.e., enthalpy controlled and entropy driven, entropy controlled and enthalpy driven, or driven favorably by both components) could be accessed by them. Particularly significant, however, was our finding that about 88% of the binding processes examined (43 of 49) involved entropy-enthalpy compensatory processes. This supports that, in these cases, binding does not result from interfaces with pre-existing complementarity but, rather, from those that are deficient at the level of either charge or shape complementarity.

Although entropy-enthalpy compensation appears to represent the principal mode by which the two germline mAbs bind to diverse Ags, it is notable that the dominating mechanism here (39 of 43 cases) is one in which significantly unfavorable changes in entropy are overcome by positive enthalpic contributions (Fig. 1, *B* and *C*). Although solvent effects may also contribute, it is pertinent that the extent of entropy control, in all the relevant bindings shown in Fig. 1, *B* and *C*, is directly dependent upon the nature of both Ab and Ag. More importantly, the association step of the binding reaction—which necessarily involves disruption of solvation at the interface (i.e., favorable entropic changes in solvent)—is also characterized by a substantial entropic penalty (Fig. 1, *B* and *C*, *insets*). Collectively, therefore, these results strongly suggest that the observed entropy control identifies conformational adaptation of the interacting interfaces. Variation in $T\Delta S_{eq}$ values, for mAb binding to independent clones, may then probably reflect variations in the degree of adaptability required (Fig. 1, *B* and *C*).

Convergence of Ab reactivities

The observed plasticity, in the interactions between each germline Ab and various phage clones, prompted us to investigate whether this property may also allow an overlap in specificities of the individual Abs. To examine for this, the mAb BBE6.12H3-reactive phage pool was subjected to further selection against the heterologous mAb 36-65. From this set, 10 independent clones, with distinct insert sequences, were taken for an analysis of binding to both mAbs 36-65 and BBE6.12H3. The protocol used was identical with that described earlier, and the results are depicted in Fig. 2.

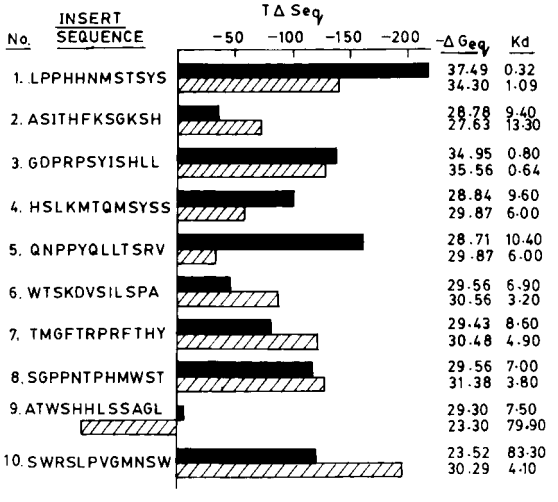

FIGURE 2. Convergence of mAb BBE6.12H3 and mAb 36-65 reactivities. The binding properties of either mAb BBE6.12H3 (■) or mAb 36-65 (▨) to a common subset of phage clones are depicted. Shown here are the $T\Delta S_{eq}$ values, along with insert sequences of the individual phage clones. In addition to this, values for the overall free energy of binding (given as $-\Delta G_{eq}$) and the equilibrium dissociation constant (K_d) at 25°C are also indicated. These values were obtained as described for Table I and Fig. 1.

All of the phage clones selected bound both mAbs BBE6.12H3 and 36-65 with affinities that were either comparable to, or significantly greater than, that for the respective homologous Ag (Fig. 2). Interestingly, with the exception of clone numbers 9 and 10, Ab binding affinities for a given phage clone were comparable (i.e., within 5-fold), suggesting the existence of shared Ag specificities by mAbs BBE6.12H3 and 36-65. Significantly, however, all of the binding interactions described were derived from entropy-enthalpy compensatory processes where, with the sole exception of mAb 36-65 binding to clone number 9, the dominant mechanism involved an unfavorable entropy component.

The energetics of individual mAb interactions with a common phage clone were, however, distinct in most of the cases and were dependent upon the nature of Ab used. This was equally true of instances in which both mAbs displayed comparable (within 5-fold) binding affinities. For example, the entropic penalty associated with mAb BBE6.12H3 binding to clones 1, 4, and 5 was significantly greater than the corresponding values for mAb 36-65 binding (Fig. 2). However, the converse was the case when interactions with clone numbers 2, 6, and 7 were compared (Fig. 2). As opposed to these two groups, binding to either clone number 3 or 8 was characterized by a relatively comparable—but not identical—degree of entropic constraint for both mAbs (Fig. 2). Finally, clone number 9 presents an interesting case where binding to mAb BBE6.12H3 was enthalpically driven, in contrast to its entropically driven interaction with mAb 36-65 (Fig. 2). Thus, the recognition of a common Ag by these structurally distinct mAbs derives from their ability to use energetically diverse binding pathways. Importantly, this also facilitates achievement of a comparable binding affinity to a given Ag in many cases.

To further improve the resolution of our analysis, we included an additional germline Ab, mAb PC7bM, in these studies. This mAb, generated from the early primary response to a peptide Ag, was of the IgM class and has been described earlier (12). For the present purposes, however, it is pertinent to mention that the Ig H chain of this mAb is composed of the V_H Q52, D_H SP2, and the J_H3 gene segments, with a HCDR3 of 10 amino acid residues. Furthermore, the L chain used by this Ab is of the κ isotype. Thus, mAb PC7bM represents a structurally distinct addition to the two mAbs that have been used so far.

The pool of BBE6.12H3 reactive phages, which had been further selected against mAb 36-65, was subjected to an additional round of panning against the monomeric form of mAb PC7bM (see *Materials and Methods*). Of the various individual clones isolated from the resultant eluate fraction, 10—all with distinct insert sequences—were taken for an analysis of their binding properties to Fab of mAb BBE6.12H3, mAb 36-65, or mAb PC7bM. The cumulative results from such experiments are presented in Table III. It is obvious that these results further extend the findings in Fig. 2. They demonstrate that convergence of Ag specificities can encompass more than two structurally distinct germline Abs. Notably, observed binding affinities were well within the range of physiological relevance, with K_d values of ~5.0 μM or less in all but two of the cases (Table III). Furthermore, for the majority of the phage clones, binding by all three mAbs occurred with comparable (within 5-fold) affinities, although the kinetic parameters contributing to this were not necessarily identical in all cases (Table III).

The data in Fig. 3 present an analysis of the energetics of mAb-phage interactions during the association step, the dissociation step, as well as under equilibrium binding conditions. A cursory examination of the association phase of the binding reaction reveals that, in all cases, this step was overwhelmingly dominated by an unfavorable change in entropy (Fig. 3). It was the net positive

Table III. *Focalized recognition of a common subset of phage clones by mAbs BBE6.12H3, 36-65, and PC7bM*[a]

		mAb BBE6.12H3			mAb 36-65			mAb PC7bM		
Clone No.	Insert Sequence	K_d (μM)	k_{ass} ($M^{-1}s^{-1}$) ($\times 10^{-5}$)	k_{diss} (s^{-1}) ($\times 10^{2}$)	K_d (μM)	k_{ass} ($M^{-1}s^{-1}$) ($\times 10^{-5}$)	k_{diss} (s^{-1}) ($\times 10^{2}$)	K_d (μM)	k_{ass} ($M^{-1}s^{-1}$) ($\times 10^{-5}$)	k_{diss} (s^{-1}) ($\times 10^{2}$)
BA7-07	SWLSHPVGMNSW	3.24	0.05	1.65	2.20	0.04	0.97	3.25	0.02	0.78
BA7-09	PPYPAWHAPGNI	0.60	0.13	0.78	0.82	0.04	0.31	0.63	0.09	0.52
BA7-01	QLADTTHHRPWT	6.11	0.03	1.78	1.62	0.04	0.61	0.53	0.12	0.60
BA7-03	ATWSHHLSSAGL	1.02	0.05	0.49	1.25	0.04	0.51	4.50	0.01	0.41
BA7-05	GAHLLSRSFASL	16.90	0.01	2.30	1.96	0.02	0.42	5.52	0.05	2.60
BA7-27	HTLKYPSSASGS	1.62	0.05	0.80	1.84	0.07	1.22	0.21	0.28	0.61
BA7-28	HSNWRVPSPWQL	4.04	0.06	2.13	1.74	0.04	0.59	0.38	0.10	0.37
BA7-31	YSPDPRPWSSRY	0.85	0.07	0.60	0.37	0.06	0.21	0.39	0.09	0.34
BA7-11	LLADTTHHRPRS	1.51	0.11	1.65	1.92	0.10	1.93	1.63	0.18	2.80
BA7-18	AHMALTYPFRPP	2.04	0.07	1.41	0.82	0.07	0.60	1.18	0.12	1.41

[a] Phage clones displaying reactivity against all three Abs are described here in terms of their corresponding insert sequences. Also given are the values for the equilibrium dissociation constant (K_d), and the kinetic rate constants for the individual Abs. These values were obtained as described for Table I.

contribution from the enthalpy component that rendered association permissive (Fig. 3). These results further support a case for structural adaptation at the paratope-epitope interface, particularly because solvent effects are not expected to contribute toward the unfavorable entropy of association (20).

Importantly, consistent with our findings in Fig. 2, binding to a given phage clone by each of the three mAbs generally involved Ab-dependent variations in the extent of the accompanying entropy control (Fig. 3). This was equally true of instances where the binding affinity eventually obtained was comparable (Figs. 2 and 3). Collectively, therefore, these results implicate that the entropic barrier to Ag binding derives, at least to a significant extent, from structural changes occurring at the level of the combining site of the respective Ab. Thus, the energetically distinct pathways used by the three mAbs, when binding to a common phage clone, presumably also reflect variations in the degree of adaptation of paratope conformation required.

The conformational space explored by independent germline Abs may vary

Given that the entropy component associated with the above binding reactions reflected—to at least some degree—the extent of structural adaptation of the paratope, we anticipated that a further examination of this parameter may yield insights into any distinctive features of these germline mAbs. Two independent selection protocols had been used in this study to screen for mAb-phage cross-reactivity. The first involved an unconstrained search, by either mAb BBE6.12H3 or mAb 36-65, through the entire antigenic repertoire provided by the phage library. After this, however, a more stringent protocol was resorted to in which selection was forced in the direction of convergent reactivities. Both of these above conditions were examined, taking data either from Tables I and II or from Table III. Because our objective was to specifically compare the degree of adaptability in binding reactions of reasonably high affinity, only those cases with a negative contribution from $T\Delta S_{eq}$ and K_d values of 10 μM or less were taken for analysis.

Fig. 4 depicts the radial distribution of negative $T\Delta S_{eq}$ values obtained for the individual mAbs under conditions where either no selection pressure was applied (Fig. 4*A*) or where selection was biased toward a common reactivity of the three mAbs (Fig. 4*B*). An interesting discrepancy can be noted between the two panels depicted in Fig. 4. In the case where no selection pressure was applied, the $T\Delta S_{eq}$ values for mAb 36-65 clustered to within a rather narrow range with most (12 of 15) falling within a value of -100 kJM^{-1} (Fig. 4*A*). In contrast to this, the corresponding values for mAb BBE6.12H3 were more widely distributed, with only 5 of 19 cases yielding $T\Delta S_{eq}$ values within -100 kJM^{-1} (Fig. 4*B*). We interpret this distinction to reflect the degree of adaptability inherent to the combining site of the respective Ab. Interestingly,

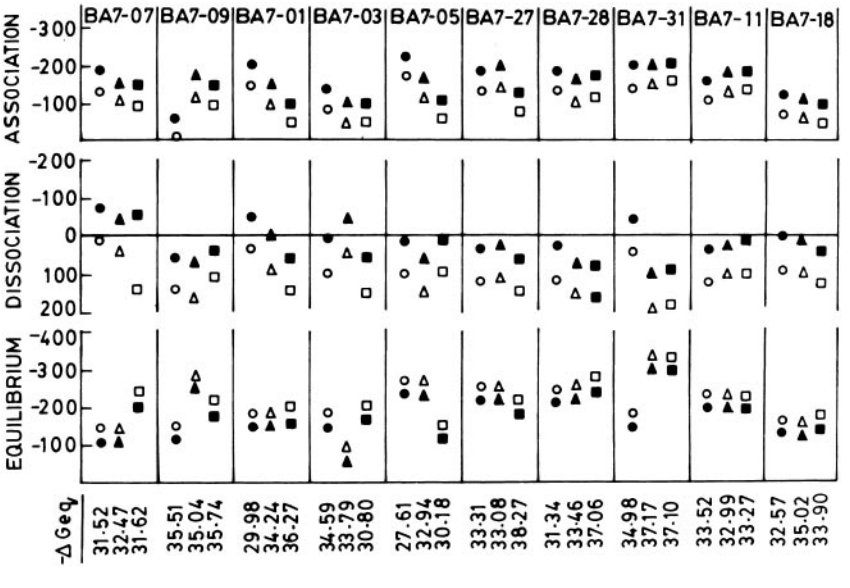

FIGURE 3. Convergent recognition of individual phage clones by mAbs BBE6.12H3, 36-65, and PC7bM. Thermodynamic parameters regulating binding by mAb BBE6.12H3 (circles), mAb 36-65 (triangles), or mAb PC7bM (squares) for the individual clones described in Table III are shown. Data are presented for both ΔH (open symbols) and $T\Delta S$ (closed symbols) during the association step (*top panel*), the dissociation step (*middle panel*), as well as under equilibrium binding conditions (*bottom panel*). The corresponding ΔG_{eq} value (presented as $-\Delta G_{eq}$) for each binding interaction is also given. These values were obtained as described for Fig. 1.

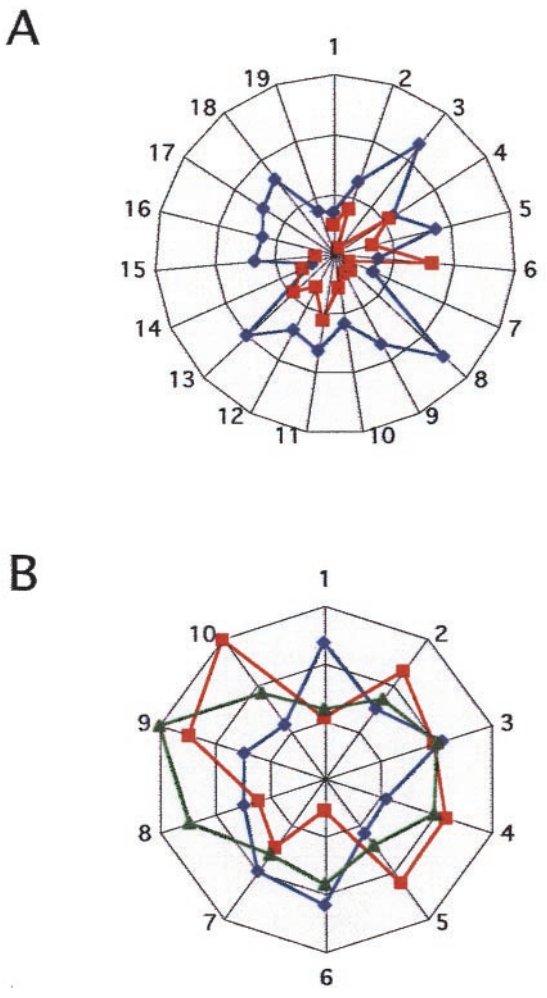

FIGURE 4. Radial distribution of $T\Delta S_{eq}$ values during phage-mAb interactions. This figure depicts the spatial distribution of the entropic penalty associated with individual mAb binding to select phage clones (see *Results*) obtained under selection conditions that were either unbiased (*A*) or directed toward convergent reactivities (*B*). The $T\Delta S_{eq}$ gradient shown is from 0 to -300 kJM^{-1}, where each concentric circle represents an increment of -100 kJM^{-1}. Each radial line is indicative of a phage clone, and the mAbs are represented as follows: BBE6.12H3, blue line; 36-65, red line; PC7bM, green line.

however, the spread of $T\Delta S_{eq}$ values obtained in Fig. 4*B* was comparable for the three mAbs 36-65, BBE6.12H3, and PC7bM. Thus, in principle, all three germline mAbs appear to be capable of being compelled to undergo similar extents of conformational adaptation. Under unconstrained conditions, however, it is obvious that mAbs 36-65 and BBE6.12H3 differ in terms of the entropic window that they naturally prefer to explore (Fig. 4*A*). In other words, when selecting from a milieu of Ags, binding by mAb 36-65 is likely to be biased toward those Ags where requisite binding affinities are achieved with only a moderate structural reorganization at the interface. In contrast, mAb BBE6.12H3 could represent a germline analogue that is more tolerant of relatively increased entropic barriers to Ag binding.

Paratope plasticity is also retained by the germline B cell receptor (BCR)

Our data obtained so far, with soluble Fab, strongly suggest that Ag recognition in a primary response occurs in a relatively degenerate fashion due to the conformational flexibility of the germline paratope. However, it remained to be formally verified whether such a binding behavior also extends to the germline BCR. To examine this, cells of the plasmacytoma line M12 were transfected with cDNA constructs of mIgD H chain and a λ L chain that also encoded the V_H and V_L gene segments, respectively, of mAb BBE6.12H3. The surface expression of mIgD$_H$-λ$_L$ receptors by the transfected cells is depicted in Fig. 5*A*. The functional integrity of these receptors could also be established by the fact that the transfected, but not the parent, cells displayed dose-dependent binding to NP-BSA as detected by flow cytometry (data not shown).

To examine the binding properties of the above receptor, we selected the phage clones described in Table III, after first labeling

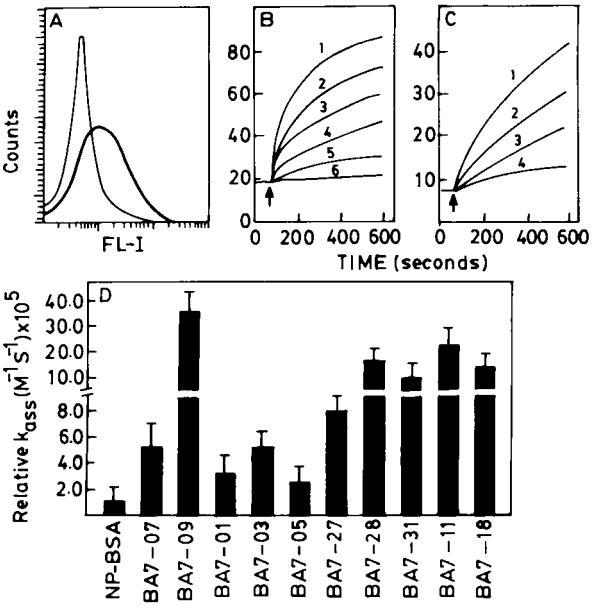

FIGURE 5. Promiscuous Ag binding by the germline BCR. *A*, Flow cytometric profile obtained after staining either untransfected (thin line) or transfected (thick line) M12 cells with FITC-labeled anti-IgD Abs. A similar profile was obtained when these cells were stained with FITC-labeled Abs to the λ isotype of the Ig L chain. *B*, Dose-dependent binding of the FITC-labeled phage clone BA7-27, as a function of time, to transfected M12 cells. For this, cells at 1.5×10^5/ml were incubated with varying concentrations of labeled phage at room temperature, and time-dependent binding was monitored by flow cytometry. The concentrations of the phage virions used were 300 nM (curve 1), 150 nM (curve 2), 80 nM (curve 3), 40 nM (curve 4), and 20 nM (curve 5). Curve 6 describes the interaction between untransfected M12 cells with a 300 nM concentration of the phage virions. The concentration of phage virions was determined by dividing the titer (i.e., PFU/liter) by the Avagadro number. Results shown are representative of three separate experiments, and the time of addition is indicated by the arrow. The binding of FITC-labeled NP-BSA to transfected M12 cells, as well as its dose-dependent inhibition in the presence of unlabeled phage BA7-27, is shown in *C*. Here, cells were incubated with a 500-nM concentration of NP-BSA at room temperature either in the absence (curve 1) or presence of increasing concentrations of the phage BA7-27, and time-dependent binding of NP-BSA to cells was monitored by flow cytometry. Phage concentrations used were 150 nM (curve 2), 300 nM (curve 3), and 600 nM (curve 4). Data presented are from one of three separate experiments, and the time of addition is indicated by the arrow. Experiments of the type described in *B* also allowed estimation of the relative association rates (relative k_{ass}) for the binding of individual phage clones, or NP-BSA, to transfected M12 cells. For this the slope of the linear portion of the individual curves (i.e., events/second) were divided by the corresponding phage (or NP-BSA) concentration to obtain the relative k_{on}. The average of the relative k_{on} values obtained at three separate concentrations of either phage or NP-BSA was then taken as the relative k_{ass}. The results thus obtained are compared in *D*, and the values given are the mean (±SD) of three independent determinations.

them with fluoroscein isothiocyanate (see *Materials and Methods*). Both transfected and untransfected M12 cells were independently incubated with varying concentrations of each of the FITC-labeled phages and time-dependent binding to the cells monitored by flow cytometry. As shown in Fig. 5*B* for a representative case, all of the phage clones tested showed dose-dependent binding to the transfected cells. The specificity of this interaction could be demonstrated by the fact that no binding to any of the phage clones could be detected when untransfected M12 cells were used instead (e.g., Fig. 5*B*). Furthermore, binding of FITC-labeled NP-BSA to transfected M12 cells could also be inhibited, in a dose-dependent manner, by the individual unlabeled phage clones. A representative example is shown in Fig. 5*C*.

By taking the slopes of the curves shown in Fig. 5*B*, we also calculated the relative association rate constants for the binding interaction between transfected M12 cells and either each of the phage clones or NP-BSA. These results are depicted in Fig. 5*D*. Although the relative association rates obtained here and the k_{ass} values of BBE6.12H3 Fab binding in Table III are not directly comparable, it is evident that the overall trend is generally maintained. More importantly, the majority of the phage clones tested bound to transfected M12 cells at relative rates that were markedly higher than that for the cognate Ag NP-BSA. This substantiates that the efficiencies of these binding interactions are well within the range of being physiologically relevant. Thus, the promiscuous binding behavior of the combining site of mAb BBE6.12H3 appears to be retained even when expressed in the context of a cell surface Ig receptor.

Discussion

Paratope plasticity and degeneracy of Ag recognition

The core finding of our present report is the pluripotential character (with respect to Ag recognition) of germline Abs. This was particularly underscored by our observations that recognition of diverse antigenic sequences, by individual germline mAbs, could be largely achieved within a relatively narrow range of binding affinities. The basis for this surprising versatility was revealed from a dissection of the thermodynamic parameters that regulated binding behavior of these Abs. Depending on the Ag encountered, they were found to be capable of adopting all thermodynamically permissive pathways, to bind the target with a reasonably high affinity. The examined interactions included cases in which binding was driven by entropy, by enthalpy, or by favorable contributions from both parameters. Importantly, the dominant binding pathway was found to involve entropy-enthalpy compensatory processes, suggesting that idealized interface complementarity was not a necessary prerequisite for binding. Although enthalpy-controlled processes reflect deficiencies in charge complementarity, those controlled by entropy identify inadequacies in shape complementarity.

The majority of the bindings observed, however, were regulated by unfavorable changes in entropy. This, in turn, defined that these interactions were mediated by substantial structural adaptation at the combining site-Ag interface, with variabilities in $T\Delta S_{eq}$ values reflecting variations in the extent to which adaptation was either achieved or required. As shown here, promiscuous binding behavior was a property restricted to germline Abs and not shared by their affinity-matured derivatives. In this connection, we have previously demonstrated that paratope plasticity also constituted a unique feature of germline Abs, including mAbs 36-65, BBE6.12H3, and PC7bM (5). As opposed to this, flexibility of the paratope in the corresponding affinity-matured derivatives was found to be severely restricted (5). Furthermore, the entropic penalty associated with independent germline mAb binding to a common phage clone was also distinctly Ab dependent. Collectively, therefore, these results suggest that the unfavorable entropy of association with Ag is, at least to a significant extent, a consequence of structural adaptations at the level of the Ab paratope.

The observed diversity, both in terms of pathways and energetics, displayed by a given Ab during binding to various Ags is inconsistent with a simple induced fit transition as originally described by Koshland (21). Rather, these findings strongly support the case for conformational polymorphism within the Ab combining site. Conformational polymorphism implies that the unbound paratope represents a distribution of diverse conformations, all existing in spontaneous equilibrium with one another (22). Each individual conformer would then provide a distinct topology for interactions with a putative ligand, thus accounting for the observed degeneracy of germline Ab binding. Furthermore, engagement of any one combining site configuration by Ag would function as a "conformation trap," shifting the equilibrium in favor of that defined in the bound form (22). The unfavorable entropy of association, and also its Ag-dependent variability, is entirely consistent with such a mechanism. Indeed, although limited, the available crystal structure data on germline Ab binding to its cognate Ag support the case for Ag-dependent modulation of paratope structure (4.6). They further reveal that both CDRH3 mobility (6) and reorientation at the V_H-V_L interface (4) can contribute to paratope adaptability.

Combining site plasticity is generally thought to be promoted by the unique architecture of the variable region, where variations in the packing of the complementarity-determining region loops against one another can provide for alternate networks of side-chain interactions (4). Indeed, substantial structural microheterogeneity can be generated by CDRH3 flexibility alone (23–25). Thus, for example, a 10-residue-long CDRH3, with a conservative assumption of three conformations per amino acid residue, may adopt as many as 3^{10} independent conformations. In reality, however, both the flanking framework regions, as well as potential noncovalent interactions with other domains, may restrict the degree of freedom to some extent. Nonetheless, consistent with its flexibility, a key role has been ascribed to the CDRH3 domain, both in terms of defining the spectrum of Ag specificities encoded within the preimmune repertoire (26) as well as in directing maturation pathways of germline Abs (27).

Although our present interpretation has favored Ab-combining site flexibility, we cannot ignore the strong likelihood that structural accommodation also occurs at the level of the Ag. Indeed, mutual adaptability at the paratope-epitope surface may well constitute the principal reason why humoral responses are frequently biased toward structurally flexible antigenic determinants (28, 29).

Polyspecific Ab reactivity has also been noted in several earlier studies. Thus, for example, naturally occurring germline Abs have been shown to cross-react with a wide variety of unrelated Ags (reviewed in Refs. 30 and 31). Interestingly, studies using combinatorial peptide libraries have revealed that affinity-matured Abs also display the ability to bind to more than one peptide epitope (32–40). In these cases, consensus motifs within the epitope sequence, however, could be identified, suggesting that such cross-reactivity derived from molecular similarity between these sequences (mimotopes) (32–40). In contrast to this, our present results are more similar to those obtained for some autoreactive Abs where the consensus motif was either more degenerate or absent (41). Thus, our study highlights, at least for the examples studied, the polyspecificity (as distinguished from cross-reactivity; see Ref. 40) of germline Abs where promiscuity derives from binding site plasticity, rather than requiring mimicry at the level of epitope.

A significant, perhaps unexpected, consequence of receptor plasticity was that it also allowed for a convergence of Ab reactivities, with binding affinities being well within the range described for primary immune responses (12, 42–44). Notably, this was predominantly supported by entropy-controlled binding pathways and required varying degrees of adaptability by the individual germline Abs. It was this finding that again highlighted the remarkable potential that conformational polymorphism can confer. Thus, three clonally independent germline Abs could use thermodynamically distinct pathways to bind to a common Ag with nearly identical affinities.

From a functional perspective, our demonstration of simultaneously existing independent (Tables I and II) as well as convergent (Fig. 2, Table III) Ag specificities, at least for mAbs BBE6.12H3 and 36-65, is also relevant. Importantly, in the overwhelming majority of both classes of interactions, the association step was nontemplated in nature (i.e., unfavorable $T\Delta S_{ass}$). Related to this is our observation that, under unconstrained selection conditions, mAb 36-65 prefers to sample a smaller area of the entropic space, relative to mAb BBE6.12H3. Collectively, then, these findings promote the view that each germline Ab represents the focus for a window of Ag specificities. The dimensions of this window may represent the thermodynamic signature of the corresponding Ab.

At one level, the existence of such windows would provide for an amplification of the recognition potential well beyond that prescribed by the BCR repertoire alone. This is experimentally supported by our demonstration that the paratope of mAb BBE6.12H3 retains its pluripotential character even when expressed in the context of a B cell surface IgD receptor. In addition to this, though, such a facility also supports, as shown here, a significant overlap in specificities of individual germline Abs. A presumable consequence of this would be the functional expression of the preimmune repertoire as a highly integrated network that could well represent an impregnable barrier for any invading Ag. Having said this, we recognize that our interpretation derives from studies with only three germline Abs. However, the fact that these Abs are markedly distinguished from each other, both in terms of their clonal origin and the Ag against which they were elicited, supports that our results are likely to be representative, rather than being system specific.

Implications for the induction and development of a primary response

From the standpoint of protecting against an invading pathogen, it is critical that both Ab induction and its subsequent maturation be rapidly achieved, before the pathogen can exert debilitating effects on the host. The felicity with which humoral responses are induced constitutes a conceptual paradox, because current estimates predict that the time taken by an Ag to scan the entire BCR repertoire would alone be of the order of several weeks (45). However, our present description of the preimmune BCR pool as a networked ensemble of degenerate Ag specificities provides a rationalization for the ready induction of humoral responses. Thus, rather than requiring an Ag to undertake an exhaustive search for the appropriate specificity, it is likely that encounter with a limited spectrum of plastic combining sites will yield a "fit" that is of a high enough affinity to induce a primary response. This latter feature would be particularly expedited by the fact that binding may also be initiated by nontemplated interactions (i.e., being initiated from noncomplementary surfaces), followed by structural reorganization at the interface. In addition to this, however, the plasticity of individual germline combining sites, as well as the structural diversity of primary Abs that a given Ag would recruit, can both be expected to contribute significantly toward the enhanced "evolvability" of the primary response (10). The increased heterogeneity of both combining site configurations and binding pathways that result is likely to favor the rapid generation of optimized variants (46–49) from only a minimized usage of the cycles of mutation and selection in germinal centers (50–54).

In summary, our results provide an important insight into both the character and functioning of the primary Ab repertoire. Whereas we experimentally confirm the existence of combining site plasticity, we also highlight that it exists to the degree that permits immune recognition to be initiated by nontemplated interactions. It is this singular feature that in one respect provides for an expanded recognition repertoire for each germline Ab and, in contrast, also creates an unpunctuated network that presumably encompasses the entire antigenic universe. From a functional context, it is again this property that is likely to ensure rapid induction of an "evolvable" primary response. Finally, we note that our present results may also shed light on how complementary surfaces—so crucial to driving all biological processes—may have evolved, starting from only a limited number of flexible templates.

Acknowledgments

We are grateful to Dr. Tim Manser for a gift of the anti-NP and anti-Ars hybridomas and to Dr. M. S. Neuberger for a gift of M12 cells. We also thank Dr. Alfred Bothwell for a critical reading of the manuscript and Pooja Chetal and Suchita Chaudhry for technical assistance.

References

1. Burnet, F. M. 1959. *The Clonal Selection Theory of Acquired Immunity*. Vanderbilt University Press, Nashville, TN.
2. Colman, P. M. 1988. Structure of antibody-antigen complexes: implications for immune recognition. *Adv. Immunol. 43:99.*
3. Paige, C. J., and G. E. Wu. 1989. The B cell repertoire. *FASEB J. 3:818.*
4. Wedemayer, G. J., P. A. Patten, L. H. Wang, P. G. Schultz, and R. C. Stevens. 1997. Structural insights into the evolution of an antibody combining site. *Science 276:1665.*
5. Manivel, V., N. C. Sahoo, D. M. Salunke, and K. V. S. Rao. 2000. Maturation of an antibody response is governed by modulations in the flexibility of the antigen-combining site. *Immunity 13:611.*
6. Mundorff, E. C., M. A. Hanson, A. Varvak, H. Ulrich, P. G. Schultz, and R. C. Stevens. 2000. Conformational effects in biological catalysis: an antibody-catalyzed Oxy-Cope rearrangement. *Biochemistry 39:627.*
7. Garcia, K. C., M. Degano, L. R. Pease, M. Huang, P. A. Peterson, L. Teyton, and I. A. Wilson. 1998. Structural basis of plasticity in T cell receptor recognition of a self peptide-MHC antigen. *Science 279:1166.*
8. Boniface, J. J., Z. Reich, D. S. Lyon, and M. M. Davis. 1999. Thermodynamics of T cell receptor binding to specific peptide-MHC: evidence for a general mechanism of molecular screening. *Proc. Natl. Acad. Sci. USA 96:11446.*
9. Wilcox, B. E., G. F. Gao, J. R. Wyer, J. E. Ladbury, J. I. Bell, B. K. Jakobsen, and P. Anton van der Meerwe. 1999. TCR binding to peptide-MHC stabilizes a flexible recognition interface. *Immunity 10:357.*
10. Joyce, G. F. 1997. Evolutionary chemistry: getting there from here. *Science 276: 1658.*
11. Mason, D. 1998. A very high level of crossreactivity is an essential feature of the T-cell receptor. *Immunol. Today 19:395.*
12. Nakra, P., V. Manivel, R. A. Vishwakarma, and K. V. S. Rao. 2000. B cell responses to a peptide epitope. X. Epitope selection in a primary response is thermodynamically regulated. *J. Immunol. 164:5615.*
13. Harlow, E., and D. Lane, eds. 1988. Reagents. In *Antibodies: A Laboratory Manual*. Cold Spring Harbor Laboratory Press, New York, p. 613.
14. Mage, M. G., and E. Lamoyi. 1987. Preparation of Fab and $F(ab')_2$ fragments from monoclonal antibodies. *Immunol. Ser. 33:79.*
15. Venkitaraman, A. R., G. T. Williams, P. Dariavach, and M. S. Neuberger. 1991. The B-cell antigen receptor of the five immunoglobulin classes. *Nature 352:777.*
16. Capra, D., C. Slaughter, E. C. B. Milner, P. Estees, and B. Tucker. 1982. The cross-reactive idiotype of A-strain mice: serological and structural analysis. *Immunol. Today 3:332.*
17. Wong, Y. H., P. H. Kussi, B. Parhami-Seren, and M. N. Margolies. 1995. Modulation of antibody affinity by an engineered amino acid substitution. *J. Immunol. 154:3351.*
18. Vora, K. A., J. V. Ravetch, and T. Manser. 1997. Amplified follicular immune complex deposition in mice: the Fc receptor γ-chain does not alter maturation of the B cell response. *J. Immunol. 159:2116.*
19. Lee, C. 1992. Calculating binding energies. *Curr. Biol. 2:217.*
20. Janin, J. 1996. Principles of protein-protein recognition from structure to thermodynamics. *Biochimie 77:497.*
21. Koshland, D. E. 1958. Application of a theory of enzyme specificity to protein synthesis. *Proc. Natl. Acad. Sci. USA 44:98.*

22. Foote, J., and C. Milstein. 1994. Conformational isomerism and the diversity of antibodies. *Proc. Nat. Acad. Sci. USA 91:10370.*
23. Chothia, C., A. M. Lesk, A. Tramontano, M. Levitt, S. J. Smith-Gill, G. Air, S. Sherrif, E. A. Padlan, D. Davies, W. R. Tulip, et al. 1989. Conformations of immunoglobulin hypervariable regions. *Nature 342:878.*
24. Chothia, C., A. M. Lesk, E. Gherardi, I. M. Tomlinson, G. Walter, J. D. Marks, M. B. Llewelyn, and G. Winter. 1992. Structural repertoire of the human V_H segments. *J. Mol. Biol. 227:799.*
25. Shirai, H., A. Kidera, and H. Nakamura. 1996. Structural classification of the CDR-H3 in antibodies. *FEBS Lett. 399:1.*
26. Xu, J. L., and M. M. Davis. 2000. Diversity in the CDR3 region of V_H is sufficient for most antibody specificities. *Immunity 13:37.*
27. Furukawa, K., A. Akasaka-Furukana, H. Shirai, H. Nakamura, and T. Azuma. 1999. Junctional amino acids determine the maturation pathway of an antibody. *Immunity 11:329.*
28. Novotny, J., M. Handschumacher, and R. E. Bruccoleri. 1987. Protein antigenicity: a surface static property. *Immunol. Today 8:26.*
29. Amzel, J. M., and B. J. Gaffney. 1995. Structural immunology: problems in molecular recognition. *FASEB J. 9:7.*
30. Avrameas, S. 1991. Natural autoantibodies: from "horror autotoxicus" to "gnothi seauton." *Immunol. Today 12:154.*
31. Notkins, A. L. 2000. Polyreactive antibodies and polyreactive B (PAB) cells. *Curr. Top. Microbiol. Immunol. 252:241.*
32. Christian, R. B., R. N. Zuckermann, J. M. Kear, L. Wang, and B. A. Malcolm. 1992. Simplified methods for construction, assessment, and rapid screening of peptide libraries in bacteriophage. *J. Mol. Biol. 227:711.*
33. Needels, M. C., D. G. Jones, E. H. Tate, G. L. Heinkel, L. M. Kochersperger, W. J. Dover, R. W. Barret, and M. A. Gallop. 1993. Generation and screening of an oligonucleotide-encoded synthetic peptide library. *Proc. Natl. Acad. Sci. USA 90:10700.*
34. De Ciechi, P. A., C. S. Devine, S. C. Lee, S. C. Howard, P. O. Olins, and M. H. Caparon. 1995. Utilization of multiple phage display libraries for the identification of dissimilar peptide motifs that bind to a B7.1 monoclonal antibody. *Mol. Divers. 1:79.*
35. Pinilla, C., J. R. Appel, P. Blanc, and R. A. Houghten. 1992. Rapid identification of high affinity peptide ligands using positional scanning synthetic peptide combinatorial libraries. *BioTechniques 13:901.*
36. Appel, J. R., J. Buencamino, R. A. Houghten, and C. Pinilla. 1996. Exploring antibody polyspecificity using synthetic combinatorial libraries. *Mol. Divers. 2:29.*
37. Demangel, C., P. Lafaye, and J. C. Mazie. 1996. Reproducing the immune response against the plasmodium vivax merozoite surface protein 1 with mimotopes selected from a phage-displayed peptide library. *Mol. Immunol. 33:909.*
38. Schnieder-Mergener, J., A. Kramer, and U. Reineke. 1996. Peptide libraries bound to continuous cellulose membranes: tools to study molecular recognition. In *Combinatorial Libraries*, R. Cortese, ed. W. de Gruyter, Berlin, p. 53.
39. Valadon, P., G. Nussbaum, L. F. Boyd, D. H. Margolies, and M. D. Scharff. 1996. Peptide libraries define the fine specificity of anti-polysaccharide antibodies to *Cryptococcus neoformans. J. Mol. Biol. 261:11.*
40. Kramer, A., T. Keitl, K. Winkler, W. Stocklein, W. Hohne, and J. Schneider-Mergener. 1997. Molecular basis for the binding promiscuity of an anti-p24 (HIV-1) monoclonal antibody. *Cell 91:799.*
41. Sibelle, P., T. Ternynck, F. Nato, G. Buttin, D. Strosberg, and A. Avrameas. 1997. Mimotopes of polyreactive anti-DNA antibodies identified using phage-display peptide libraries. *Eur. J. Immunol. 27:1221.*
42. Cumano, A., and K. Rajewsky. 1986. Clonal recruitment and somatic mutation in the generation of immunological memory to the hapten, NP. *EMBO J. 5:2459.*
43. Sharon, J. 1990. Structural correlates of high affinity antibody: three engineered amino acid substitutions can increase the affinity of an anti-*p*-azophenylarsonate antibody 200-fold. *Proc. Natl. Acad. Sci. USA 87:4814.*
44. Taketani, M., A. Naitoh, N. Motoyama, and T. Azuma. 1995. Role of conserved amino acid residues in the complementarity determining regions on hapten-antibody interaction anti-(4-hydroxy-3-nitrophenyl)acetyl antibodies. *Mol. Immunol. 32:983.*
45. Langman, R. E., and M. Cohn. 1999. Away with words: commentary on the Altan-Cohen essay "Immune Information, Self-Organization and Meaning." *Int. Immunol. 11:865.*
46. Wilson, I. A., and R. L. Stanfield. 1994. Antibody-antigen interactions: new structures and new conformational changes. *Curr. Opin. Struct. Biol. 4:857.*
47. Xu, J., Q. Deng, J. Chen, K. N. Houk, J. Bartek, and I. A. Wilson. 1999. Evolution of shape complementarity and catalytic efficiency from a primordial template. *Science 286:2345.*
48. Yang, P. L., and P. G. Schultz. 1999. Mutational analysis of the affinity maturation of antibody 48G7. *J. Mol. Biol. 294:1191.*
49. Chong, L. T., Y. Duan, L. Wang, I. Massova, and P. A. Kollman. 1999. Molecular dynamics and free-energy calculations applied to affinity maturation in antibody 48G7. *Proc. Natl. Acad. Sci. USA 96:14330.*
50. Nossal, G. J. V. 1994. Differentiation of the secondary B lymphocyte repertoire: the germinal center reaction. *Immunol. Rev. 137:173.*
51. Kelsoe, G. 1995. In situ studies of the germinal center reaction. *Adv. Immunol. 60:267.*
52. Liu, Y.-J., and C. Arpin. 1997. Germinal center development. *Immunol. Rev. 156:111.*
53. Liu, Y.-J., O. de Bouteiller, and I. Fugier-Vivier. 1997. Mechanism of selection and differentiation in germinal centres. *Curr. Opin. Immunol. 9:256.*
54. Manser, T., K. M. Tumas-Brundage, L. P. Casson, A. M. Guisti, S. Hande, E. Notides, and K. A. Vora. 1998. The role of antibody variable region hypermutation and selection in the development of the memory B cell compartment. *Immunol. Rev. 162:182.*